LBIC INVESTIGATIONS OF MULTICRYSTALLINE SILICON SOLAR CELLS WITH THE FRONT CONTACT ON GRAIN BOUNDARIES

V. Schlosser[1], R. Ebner[2], J. Summhammer[2], P. Bajons[1], G. Klinger[3]
[1]Institut für Materialphysik, Fakultät für Physik, Universität Wien, Strudlhofg 4, A-1090 Wien, Austria,
email: viktor.schlosser @univie.ac.at
[2]Vienna University of Technology, Atominstitut, Stadionallee 2, A-1020 Wien, Austria, email: summhammer@ati.ac.at
[3]Institut für Meteorologie und Geophysik, Universität Wien, Althanstr.14, A-1090 Wien, Austria,
email: img-wien@univie.ac.at

ABSTRACT: The spatial variation of locally generated photocurrents has been mapped for multi crystalline silicon solar cells equipped with two different kind of front metal grids. To a portion of the 100 mm × 100 mm solar cells the standard H-pattern with straight metal lines and two busbars was applied. The other cells were equipped with a front grid located on grain boundaries. The light beam induced current (LBIC) set-up works with two fibre coupled luminescence diodes at centre wavelengths of 655 nm and 870 nm respectively. The two light emitting diodes (LEDs) were driven by the same current and individually intensity modulated. A feedback loop for the LED current maintained a constant photocurrent arising from the red LED. The cell current caused by the infrared LED was recorded as a function of the light spot position on the solar cell. The solar cells were investigated under different electrical bias conditions using a low intensity white light background illumination of the whole cell. With the experimental set-up we were able to separate electrical and optical inhomogenities of the surface from the local electrical bulk properties.
Keywords: Multi-Crystalline, Silicon, LBIC

1 INTRODUCTION

Industrial solar cells are large area junctions. The performance, lifetime and reliability depend strongly on structural and process induced defects. Multi crystalline silicon (mc-Si) made by a directional solidification method yields large grained wafers with locally inhomogeneous sometimes very high defect densities [1]. During the preparation of mc-Si cells different crystal orientations as well as the region between the grains which has an extremely high density of lattice defects causes inhomogeneous chemical surface treatment and different doping conditions during diffusion steps. In the final solar cells especially the grain boundaries exhibit unwanted electrical characteristics. They tend to have a high concentration of electrically active defects which cause high recombination for minority carriers thus reducing the collection efficiency of light generated carriers [2, 3]. Furthermore grain boundaries often act as potential barriers for majority carriers which introduces an additional contribution to internal power losses of the solar cell [4]. Therefore cells of mc-Si suffer from lower conversion efficiencies and batches of cells have larger dispersion of the electrical parameters compared with monocrystalline Si cells. In order to minimise grain boundary effects on the solar cell performance electrically active defects are passivated by the introduction of atomic hydrogen frequently in combination with a thermal treatment to getter metallic impurities [5]. Recently an other approach to minimise efficiency losses due to grain boundary effects was suggested [6]. The metal grid of the front contact of a mc-Si solar cell was applied mainly above grain boundaries. Previously a statistically elaborated study reported an increase of the output power between 3-8 % [7]. The main reasons for this improvement were found to be the lowered series resistance and the reduced recombination in the bulk, due to the fact that the front metal grid covered grain boundaries and thus opened good cell volume for light to current conversion. This method requires the individual identification of the wafer's grain structure for the evaluation of a suitable contact pattern and non destructive, local characterisation tools in order to transfer the process from laboratory to industry.

Several techniques have been proposed to locate electrically active defects in solar cells. EBIC (electron beam induced current) and LBIC (light beam induced current) techniques measure the variation of the induced current under local electron or photon beam excitation at the surface of the solar cell and are widely used today [8]. Mere optical techniques like microwave detected photocurrent decay or infrared thermography [9] are advantageous for in line characterisation since they do not require electrical contacts. However they strongly depend on optical and electrical surface properties. Therefore it is difficult to analyse the local bulk properties of minority carriers. In this work we use a modified LBIC mapping set-up to investigate cells with the improved grain boundary contacting grid and of cells equipped with the standard H-pattern under different light and temperature conditions.

2 EXPERIMENTAL

The starting material for the preparation of solar cells were p-type mc-Si wafers as delivered from Bayer or Eurosolare. The wafer surfaces were chemically polished and cleaned either by an acetic or by a hydroxide solution. The planar pn-junction was formed by a phosphorous diffusion. The back side of all cells was fully metalised by screen printing a paste containing aluminium and silver particles. For one part of these cells the surface structure was determined by an optical contrast image which was transferred to a computer. A program starts from an initial grid with rectangular lines defined by the user's input of the desired grid parameters such as line spacing, total line length and percentage of the cell area which shall be covered by the metal. Based on the information of the optical contrast image the program distorts the initial grid layout towards a grid which still maintains the inputted parameters but is located predominately along boundaries. Currently two methods to apply the front grid are in use: (1) A Silver ink is plotted onto the

grain boundaries according to the computer driven plot instructions and then burnt in or (2) a masked photoresist covers the wafer's surface leaving regions uncovered where the metal is intended to be deposited by an electrochemical deposition from a liquid solution.

The partly processed solar cells were mounted on a computerised XY stage and connected to a power supply which was capable to serve as current sink. A heating plate beneath the device under test allowed us to maintain the measurements at a constant temperature in the range between 290 K and 350 K. Two tungsten halogen lamps were used to illuminate the whole cell with a white bias light. The LBIC mapping was done by scanning a focused light spot caused by two intensity modulated luminescence diodes, LEDs, with centre wavelengths, λ, at 655 nm and 870 nm respectively over the cell surface. Both LEDs were electrically connected in series and driven by the same current. At a current of 20 mA the output power of the visible (red) LED was about 350 µW and the output power of the IR LED was somewhat greater than 300 µW. Between 3 mA and 20 mA both emitted intensities vary linearly with current. The modulation was done by individually short circuiting the LEDs with two MOS transistors which were operated at different frequencies. The light of both LEDs was coupled into a common plastic fibre and focused on the sample's surface by a motorised lens optics. Due to cell bending caused by the screen printed back contact and a textured surface the light spot could easily run out of the focus plane. Therefore focus was permanently computer controlled and adjusted during a scan. For the two wavelengths the values for the reflection of an optically polished surface, R, index of refraction, n, and the penetration depth of light expressed by the inverse absorption coefficient, α^{-1}, for crystalline silicon at 300 K is tabulated in table I.

Wavelength, λ	655 nm	870 nm
R	34.5 per cent	32.4 per cent
N	3.84	3.65
α^{-1}	3.4 µm	29 µm

Table I: Optical properties of crystalline silicon

By the use of two Lock In amplifiers, LIAs, the total light generated current from the photovoltaic device was split into its two AC components rejecting the contribution from the white DC bias light. The experimental set-up is schematically shown in Fig. 1.

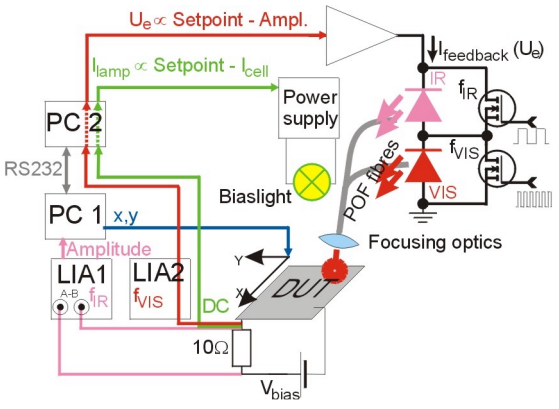

Figure 1: Schematic diagram of scanning LBIC system.

As can be seen from table I the reflection and the index of refraction at 870 nm differ only by about 5 per cent from the values of the red light. The inverse absorption coefficient however is about one order of magnitude larger for the IR light beam. The photocurrent induced by the red LED is governed by the local optical properties of the surface and by the electrical properties of the photoexcited minority carriers close beneath the surface predominately in the highly doped emitter region. The signal induced by the IR LED depends almost in the same way by the optical surface properties. The region of photoexcited carriers contributing to the total light beam induced current however extends into the base of the solar cell. Instead of recording the two photoexcited signals for a constant LED current as a function of the light spot position on the solar cell a feed back loop for the LED current was used maintaining a constant LBIC signal arising from the red LED. The LED's current and the signal induced by the IR illumination was recorded as a function of the light spot position. By doing so the IR LBIC signal is nearly free from optically introduced variations due to local surface inhomogenities caused by surface texture or by surface contamination. Furthermore the influence of electrically active defects located in the highly doped emitter region on the resulting IR LBIC signal is significantly lowered thus enhancing the deep

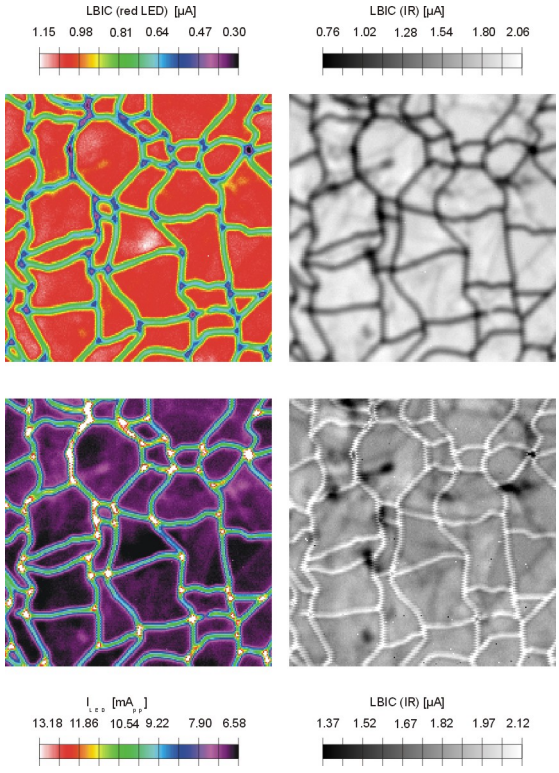

Figure 2: Comparison of two LBIC scans with two different wavelengths. The top row shows the local LBIC for red excitation (left) and IR excitation (right) for a constant drive current of both LEDs. The bottom row shows the current for both LEDs necessary to maintain a constant signal from the red LED (left) and the LBIC map for th IR excitation (right).

lying defects in the base region of the solar cell. In Fig. 2 a comparison of a LBIC scan for a 4 cm × 4 cm area of a mc-Si cell with grain boundary front contacts is shown. In the first case the drive current for both LEDs was kept constant which is equivalent to constant incident light intensities of both LEDs. In the second case the feedback loop adjusts the red LBIC to a predefined setpoint which means that the incident light intensities vary with light spot position on the sample. At constant light intensities as shown in the upper two images of Fig. 2 a high signal indicates a locally high external quantum efficiency. Regions which are shaded by the metal grid of the front contact appear dark since the external quantum efficiency is zero because the metallic reflection is 100 per cent. The LBIC map for the red excitation (upper left image in Fig. 2) is similar to the one for the IR excitation (upper right image in Fig. 2). Since both, a locally higher optical reflection and a higher density of electrically active defects are displayed in the same way by a lower value of the colour scale it is difficult to distinguish between these two effects. When the LBIC set-up is operated in the feedback loop mode the diode current is mapped as a function of the surface position which is shown in the lower left image of Fig. 2. Since the emitted intensities of both LEDs vary linearly with the drive current for the range of operation between 5 mA and 20 mA as has been mentioned above the map displays the local red light intensity necessary to maintain a constant photocurrent. Regions which are completely shadowed by the metal grid would force the feedback loop to an infinite high current which is experimentally limited to 20 mA. The lower left image appears inverted to the upper left image which means that cell regions with a locally low concentration of electrically active defects are indicated by dark areas. Optically shaded areas are displayed in colours at the upper end of the colour scale. The right image shows the local photocurrent from the IR excitation in the case that the incident light intensity varies according to the feedback loop. In comparison with the upper right image a better grey scale contrast is observed. Locally lowered values of the photoexcited minority carrier diffusion length due to electrically active defects appear dark and are mainly located in the base region of the photovoltaic device. Surface near defects will strongly affect the red LBIC signal which forces the feedback loop to increase the emitted IR intensity which will result in a low or even no contrast of the scanned IR LBIC image. Although optical shadowing should result in dark colours in the image the contacted grain boundaries appear as almost white lines. This is caused by the integration time of the Lock In amplifier for the IR signal detection which in this case responds to a change of the signal too slow. That means that depending on the integration times of the Lock In amplifiers, the response time of the feedback loop and the scan speed the IR LBIC image can be displaced compared with the intensity plot along the scan direction.

In order to operate the solar cell in a well defined manner during the scan it is connected to a power supply which is capable to act as an electronic load and the solar cell is kept at a constant bias voltage either in reverse polarity acting as light sensitive diode or at low forward voltages between 0 and open circuit voltage, V_{OC}, during the scan. V_{OC} was depending on the white bias light illumination. The presence of optics for the light beam partially shadows the solar cell from the white bias light coming from two lamps. Therefore the induced DC photocurrent of the photovoltaic device can change when the optics position changes relative to the cell since different cell regions are shadowed. This problem could not be completely suppressed during a whole scan by rearranging the light bulbs. Therefore the white light irradiation was varied during the LBIC recording thus keeping the cell's current excited by the bias light constant.

3 RESULTS AND DISCUSSION

In Fig. 3 and Fig. 4 results from a scan made on a mc-Si solar cell with the front contact grid placed on the

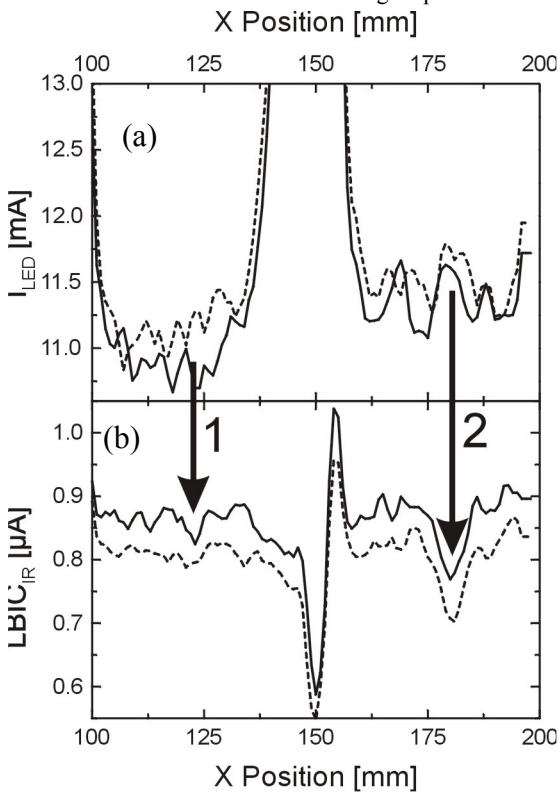

Figure 3: Plot of the irradiated intensity (a) and IR LBIC (b) as a function of the position for a solar cell which was illuminated with ~10 mWcm^{-2} and kept at 304 K while operated in reverse polarity (solid line) and forward polarity (dashed line).

grain boundaries are shown. Both figures display a portion of a single line of the same scan. In Fig. 3 the scan direction was along the line. The light spot was moved in the direction of increasing position. In Fig. 4 the plot is perpendicular to the scan direction. The scans were taken for modulation frequencies of 5.82 kHz for the red LED and 0.513 kHz for the IR LED. The integration time constants of the Lock In amplifiers were 30 ms for the red LBIC detection and 100 ms for the IR LBIC detection. At the horizontal centre of Fig. 3 (about 150 mm in X direction) light beam travels over a metal grid line. The drive current and thus the LED intensities increases rapidly with increasing position as can be seen in Fig. 3a. Due to the higher integration constant for the recording of the IR signal the LBIC response appears delayed with

increasing position. Therefore the LBIC signal does not reach zero. Moving the light spot towards larger positions the feedback loop decreases the drive current of the LEDs too slow for the selected light spot motion, therefore the IR LBIC overshoots on the right side of the contact. Despite these imperfections of the system a minimum of the IR LBIC was detected which appears solely at reverse bias conditions marked with arrow 1 in Fig. 3. It remains invisible in the intensity plot and was not found for forward voltage conditions. Therefore we conclude that it is caused by an electrically active defect in the base region of the solar cell. The position marked by arrow 2 indicate a change of the signals that is visible in both plots and independent of the bias voltage. It is very likely that this was caused by an electrical defect which extends from the base region to the surface of the device. Arrow 3 in Fig. 4 indicates a maximum in the emitted light intensities of the LEDs which does not have any effect on the IR LBIC signal. The origin is potentially a surface contamination due to insufficient cleaning which reduced the optical reflection.

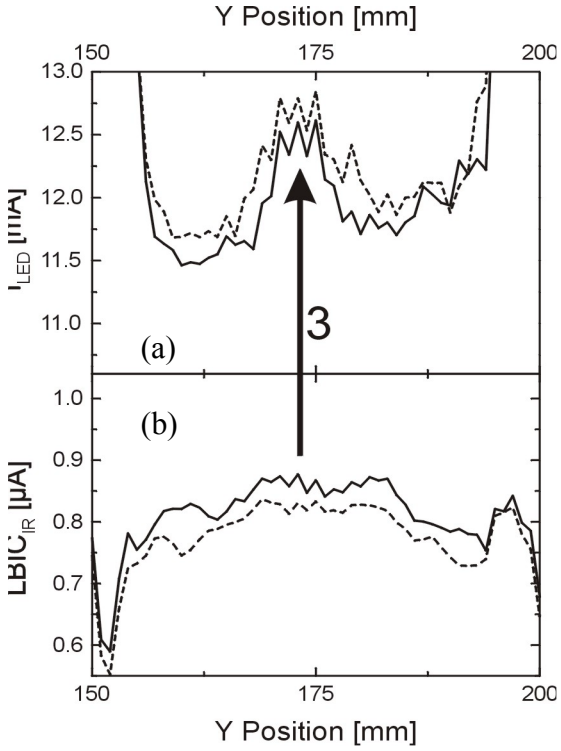

Figure 4: Plot of the irradiated intensity (a) and IR LBIC (b) as a function of the position for a solar cell which was illuminated with ~10 mWcm^{-2} kept at 304 K and operated in reverse polarity (solid line) and forward polarity (dashed line).

4 CONCLUSIONS

We have demonstrated that the use of two fibre coupled light emitting diodes combined with a Lock In amplifier detection technique of the light generated local currents and a feedback loop offers an easy way to identify the origin of different contributions to the local photocurrent. The quality of the LBIC and intensity mapping depends strongly on the proper settings of (i) intensity modulation frequencies and signal integration time constants (ii) the time constant of the feedback loop and (iii) light spot motion speed. For a given system these parameters can be either optimised for scan speed capable for fast inline characterisation or for sensitivity thus allowing to extract local minority carrier parameters such as lifetime and surface recombination velocity at grain boundaries by detailed analysis of the recorded signals.

REFERENCES

[1] C. Häßler, G. Stollwerk, W. Koch, W. Krumbe, A. Müller, Proc.16th European Photovoltaic Solar Energy Conference (Glasgow, May 2000).
[2] J. Y. W. Seto, J. Appl. Phys. **46**, 5247-5254 (1975).
[3] S. A. Edmiston, G. Heiser, A. B. Sproul, and M. A. Green, J. Appl. Phys. **80** 6783-6795 (1996).
[4] P. T. Landsberg, and M. S. J. Abraham, Appl. Phys. **55**, 4284-4293 (1984).
[5] D. Macdonal, and A. Cuevas, Sol. Energ. Mat. Sol. C. **65**, 509-516 (2001).
[6] J. Summhammer, and V. Schlosser, "Investigations of a novel front contact grid on poly silicon solar cells" in Proceedings of the twelfth European Photovoltaic Solar Energy Conference, edited by H. A. Ossenbrink et al., Bedford, UK: H.S. Stephens and Associates, 1994, pp. 734-737.
[7] R. Ebner, M. Radike, V. Schlosser, and J. Summhammer, Prog. Photovolt: Res. Appl. **11**, 1-13 (2003).
[8] A Kaminski, O. Breitenstein, J. P. Boyeaux, P. Rakotoniana and A. Laugier, J. Phys: Condens. Matter, **16**, S10-S18 (2004).
[9] O. Breitenstein, M. Langenkamp, O. Lang, A. Schirrmacher, Sol. Energ. Mat. Sol. C. **65**, 55-62 (2001).